CHEMISTRY & SUSTAINABILITY

CHEMSUSCHEM

ENERGY & MATERIALS

Accepted Article

Title: Selective aerobic oxidation of 5-(hydroxymethyl)furfural to 2,5-diformylfuran or 2-formyl-5-furancarboxylic acid in water using MgO·CeO2 mixed oxides as catalysts

Authors: Angela Dibenedetto, Maria Ventura, Francesco Lobefaro, Elvira de Giglio, Monica Distaso, and Francesco Nocito

To be cited as: *ChemSusChem* 10.1002/cssc.201800334

Link to VoR: http://dx.doi.org/10.1002/cssc.201800334

A Journal of

ChemPubSoc Europe

WILEY-VCH

www.chemsuschem.org

10.1002/cssc.201800334

WILEY-VCH

FULL PAPER

Selective aerobic oxidation of 5-(hydroxymethyl)furfural to 2,5-diformylfuran or 2-formyl-5-furancarboxylic acid in water using $MgO{\cdot}CeO_2$ mixed oxides as catalysts

Maria Ventura,[b] Francesco Lobefaro, [c] Elvira de Giglio,[a] Monica Distaso, [d] Francesco Nocito, [a] and Angela Dibenedetto*[a,b]

Abstract: Mixed oxides based on $MgO{\cdot}CeO_2$ were used, as efficient catalysts, in the aerobic oxidation of 5-(hydroxymethyl)furfural (5-HMF) to afford, with very high selectivity, either 2,5-diformylfuran (DFF, 99%) or 2-formyl-5-furancarboxylic acid (FFCA, 90%) depending on the reaction conditions. 5-Hydroxymethyl-2-furancarboxylic acid (HMFCA, 57-90%) was formed only at low concentration of 5-HMF (<0.03 M) or in presence of external bases. The conversion of 5-HMF ranged from a few units to 99 %, according to the reaction conditions. The oxidation was performed in water, with O_2 as oxidant, without any additives. The surface characterization of the catalysts gave important information about their acid-base properties, which drive the selectivity of the reaction towards DFF. FFCA was formed from DFF for longer reaction times. Catalysts were studied by XPS and XRD before and after catalytic runs to identify the reason why they undergo reversible deactivation. XRD has clearly shown that MgO is hydrated to $Mg(OH)_2$ which, even if not leached out, changes the basic properties of the catalyst that becomes less active after some time. Calcination of the recovered catalyst allows recovering their initial activity. The catalyst is, thus, recoverable (>99%) and reusable. The use of mixed oxides allows tune the basicity of catalysts, avoiding external bases for efficient and selective conversion of 5-HMF and waste formation, resulting in an environmentally friendly, sustainable process.

Introduction

Over the last decades the depletion of fossil fuel resources and the increased atmospheric CO_2 level,[1] have forced to investigate how to replace fossil carbon with renewable carbon, such as biomass or even CO_2. 5-(Hydroxymethyl)furfural (5-HMF), a furan ring bearing an aldehyde and a hydroxyl moiety, is obtained from glucose by isomerization to fructose under basic catalysis and subsequent dehydration of the latter in acidic conditions (Scheme 1).[2] It has been identified as an important platform chemical with high industrial potential as intermediate feedstock.[3]

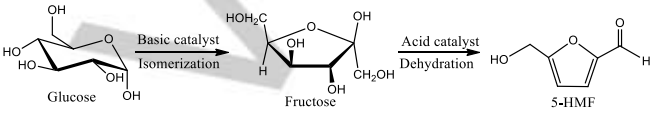

Scheme 1. Reaction pathway for the synthesis of 5-HMF from glucose.

As shown in Scheme 2, 5-HMF can undergo oxidation to different products. In particular, the oxidation of the aldehyde group leads to 5-hydroxymethyl-2-furancarboxylic acid (HMFCA), while the selective oxidation of hydroxyl moiety produces the furan dialdehyde 2,5-diformylfuran (DFF). Oxidation of the latter two compounds leads to 5-formyl-2-furancarboxylic acid (FFCA), precursor of 2,5-furandicarboxylic acid (FDCA).

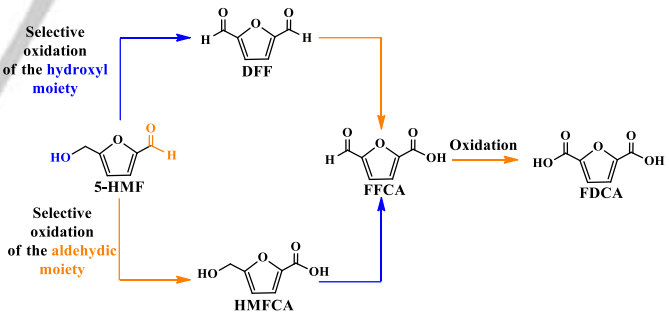

Scheme 2. The pathway of 5-HMF oxidation to DFF, HMFCA, FFCA and FDCA.

DFF is a versatile chemical intermediate for the synthesis of pharmaceuticals,[4] fungicides,[5] furan-urea resins[6] or heterocyclic ligands.[7] Several reports describe the formation of DFF in organic solvents,[8] despite the use of the latter contributes to the formation of waste in the whole process.[9] Even photocatalytic systems have been used[9b] or metal-free processes[9c,d] or oxidant-free catalytic systems.[9e] Expensive metals, such as ruthenium or gold, have often been used as catalysts.[10] Recent studies have shown that DFF can be synthesized in water with good conversion and 87% selectivity, when $Mn_{0.70}Cu_{0.05}Al_{0.25}OH$ was used as catalyst in mild conditions in absence of any additives. The structural properties

[a] Prof. A. Dibenedetto, Prof. E. de Giglio, Dr F. Nocito
Department of Chemistry,
University of Bari, Campus Universitario, 70126 Bari, Italy
E-mail: angela.dibenedetto@uniba.it
[b] Prof. A. Dibenedetto, Dr M. Ventura
CIRCC, Via Celso Ulpiani, 27, 70126 Bari, Italy
[c] MSc F. Lobefaro
IC²R, Tecnopolis,
km 3 via Casamassima, 70018 Valenzano (BA), Italy
[d] Dr M. Distaso
Institute of Particle Technology (LFG)
Cauerstrasse 4D-91058, Erlangen, Germany.

of the catalysts have not been fully disclosed, and this leaves unclear the justification of such high activity.[11] To the best of our knowledge, there are no other reports describing a comparable selectivity towards DFF using water as solvent and homogeneous or heterogeneous catalysts. In fact, metal systems such as Cu(II), Fe(II), Cu(II) with SALEN ligand afforded 14.39% selectivity, using H_2O_2 as oxidant.[12] 13.3% selectivity was reached when Ru was supported on poly(4-vinylpyridine)-functionalized Carbon NanoTubes (CNT).[13] Conversely, covalent triazine frameworks-CTF[14] enhance the selectivity up to 52%, while oxidation to FFCA also takes place. Over activated carbon, a selectivity of 60.5%[10a] and 28.8%[15] is reported. γ-Al_2O_3 or CeO_2 allow to reach selectivity of 37.5%[10b] and 18%,[16] respectively. Such large variety of data gives an idea of how important are both the catalyst and the support in this kind of oxidation reaction.[16] Studies of catalytic systems based of N-hydroxyphthalimide with ceria show that increasing the amount of ceria produces different results. For instance, the use of large amount of CeO_2 causes a decrease of selectivity.[17] Au[18] or Cr[19] were also used but no more than 30% of selectivity was reached. Even if recently the synthesis of FDCA with excellent yield and selectivity has been reported,[20] good yields or selectivity of DFF, which is the intermediate in the FDCA synthesis (Scheme 2), is still matter of research. Besides the catalyst, also the solvent and the oxidant play a key role. In principle, the use of water as well as the use of O_2 should minimize the waste formation and make the process more environmentally friendly. Noteworthy, when the target product is DFF, reactions in water are difficult to control. In fact, pH also plays a key role in the reactivity of 5-HMF and its derivatives. In Scheme 3a the reactivity of 5-HMF and DFF in aqueous slightly-basic or neutral media is shown, while Scheme 3b shows the reactivity of 5-HMF in a strong basic medium. The first step in the pathway of DFF formation from 5-HMF is the alcohol activation (Scheme 3a). In slightly basic aqueous solutions (or in presence of solid basic Lewis catalysts in water) the alcoholic functionality can be easily deprotonated to its conjugate base that favours the oxidation, while at neutral or acidic pH, the equilibrium is shifted towards 5-HMF, and the oxidation of the alcoholic moiety is not favored. On the other hand, in strong basic media, the aldehyde moiety of 5-HMF is hydrated, and its oxidation is favored, achieving HMFCA (Scheme 3b). DFF shows the same behavior: in a strong basic medium it can be hydrated and FFCA is formed, while in an acidic medium such equilibrium is shifted towards DFF (Scheme 3a). Therefore, the most effective way to activate the hydroxyl group promoting the formation of DFF is the use of Lewis bases because strong Broensted bases promote also the aldehydic moiety hydration, enhancing the formation of FFCA from DFF or the formation of HMFCA from 5-HMF, with loss of selectivity.[21]

Targeting high conversion and selectivity in the absence of soluble bases, using Earth crust abundant heterogeneous catalytic systems (recoverable and reusable), in water with O_2 as oxidant is, thus, a challenging task, but a success would enable the development of environmentally safe and sustainable processes.

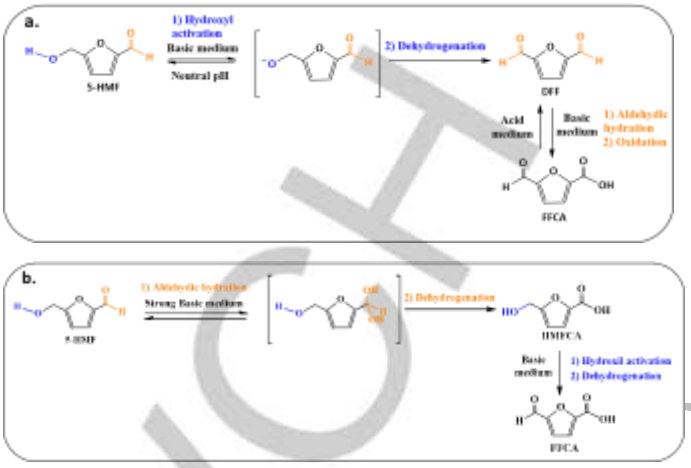

Scheme 3. Reactivity of 5-HMF in aqueous media: *a.* Activation of the alcoholic functionality in slightly basic or neutral media; *b.* Activation of aldehydic moiety in strong basic media.

Taking all such aspects into consideration, we have figured out that a bi-functional metal oxide with the correct oxidizing power and combination of basic and acidic sites would be an effective and efficient catalyst. Noteworthy, high selectivity plays an important role as it would both minimize the post reaction separation costs (energetic and economic) and reduce waste formation. However, based on our knowledge of the oxidation of 5-HMF to FFCA using tunable mixed oxides,[22] we have investigated the factors that can maximize the oxidation of 5-HMF to DFF (or FFCA), suppressing the formation of HMFCA, that implies the oxidation of aldehyde moiety instead of the alcoholic moiety. We describe here, the selective (98%+) and quantitative (99%) oxidation of 5-HMF to DFF in water with O_2 as oxidant, using magnesium/cerium mixed oxides as catalysts. We recall that physical mixtures of oxides show unpredictable and serendipitous properties.

Results and Discussion

1. Characterization of the catalysts

Table 2 shows the BET surface area and the weak and strong basic and acidic sites (calculated from the area under the peaks in the TPD experiments) of solids, expressed through the volume of CO_2 and NH_3 up-taken and released, respectively. The strength of different basic/acidic sites can be divided into three categories.[23] Using CO_2 as probe gas, peaks appearing in the temperature region of 350-430 K belong to the interaction with hydroxyl groups on the surface that are weakly basic in nature. Basic sites of medium strength are found in the temperature range of 430-670 K that are attributed to the presence of M=O moieties. The strongest basic sites are observed above 670 K and are attributed to isolated O^{2-} species. To simplify the analysis, we have merged together medium and strong sites that should be responsible of the catalytic activity, excluding weak sites.

Concerning the acidity, weak acidity is that belonging to the protons of the –OH groups on the surface, while strong acidity is relevant to the Lewis acid centers M^{n+}.[24] The lowest strong acidity was found for MgO followed by CeO_2, while the new mixed oxide $MgO{\cdot}CeO_2$ exhibits the highest value (Table 1, Entry 3; 2.51 mL g^{-1}). It is worth to mention that CeO_2 presents the highest value for the weak acidity.

Table 1. BET surface area and basicity/acidity strength of binary and ternary metal oxides

	cat	Total VCO_2 ads (mL/g)	Weak CO_2 ads (mL/g)	Strong CO_2 ads (mL/g)	Total VNH_3 ads (mL/g)	Weak NH_3 ads (mL/g)	Strong NH_3 ads (mL/g)	BET surf area (m^2/g)
1	MgO	2.21	0.24	1.97	0.93	0.09	0.85	41.35
2	CeO_2	2.34	1.01	1.32	3.05	1.26	1.80	66.12
3	$MgO{\cdot}CeO_2$	3.06	0.29	2.77	3.21	0.69	2.51	66.62

Note: a binary oxide is composed of two different elements (MO or M_2O); a ternary oxide is composed of three different elements (MM'O) (IUPAC Nomenclature).

A comparison between single oxides and mixed oxide $MgO{\cdot}CeO_2$ reveals a quite different basicity that increases in the order: CeO_2<MgO<$MgO{\cdot}CeO_2$. Interestingly, the mixed oxide $MgO{\cdot}CeO_2$ exhibits the highest strong adsorption of CO_2 (Table 1, Entry 3). CeO_2 shows the highest weak CO_2 adsorption. The BET surface area has the highest value in the case of the 1:1 mixed oxide and results to be quite close to the value proper of CeO_2. Other mixed oxides with variable Mg/Ce molar ratio were also synthesized (vide infra). Table 2 shows their BET surface area and basic/acid properties: increasing the MgO content in the mixed oxide leads to an expected increase of the basicity. The total volume of CO_2 adsorbed increases gradually while increasing the strong basic sites, at the same time the number of weak adsorption sites for CO_2 decreases as the MgO content increases.

Concerning the BET surface area, we have observed an increase with the amount of Mg until the ratio Mg:Ce reaches the value of 1, then a decrease was observed.

Table 2. Basicity/acidity strength and BET surface area of $xMgO{\cdot}CeO_2$

	Cat	Total V CO_2 ads (mL/g)	Weak CO_2 ads (mL/g)	Strong CO_2 ads (mL/g)	Total V NH_3 ads (mL/g)	Weak NH_3 ads (mL/g)	Strong NH_3 ads (mL/g)	BET surf area (m^2/g)
1	$0.1MgO{\cdot}CeO_2$	1.84	0.72	1.12	3.45	0.57	2.93	17.30
2	$0.5MgO{\cdot}CeO_2$	2.41	0.58	1.83	2.99	0.39	2.59	53.75
3	$1MgO{\cdot}CeO_2$	3.06	0.42	2.64	3.21	0.69	2.51	66.62
4	$2.2MgO{\cdot}CeO_2$	3.68	0.38	3.30	1.93	0.55	1.37	48.09

The XRD analysis of $MgO{\cdot}CeO_2$ (Fig. 1, C) shows the reflections of both CeO_2 and MgO, indicating that a solid solution of the two materials is obtained. These results are in agreement with data previously reported in the literature, whereby the solubility of Group 2 metal oxides in CeO_2 has been reported upon thermal treatment at 1673-1873 K,[25] whereas the solubility of CeO_2 in MgO has been found to be negligible.[26] In the present work, milder conditions are used by coupling HEM and calcination at 783-983 K.

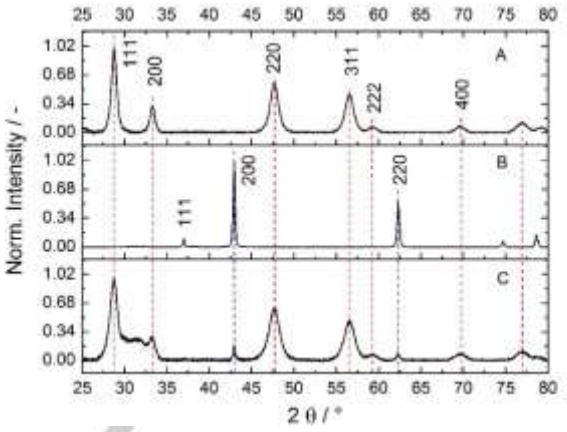

Figure 1. XRD of (A) CeO_2 (B) MgO and (C) $MgO{\cdot}CeO_2$. Dashed vertical lines indicate the reflections of CeO_2 (red) and MgO (blue), respectively, and serve as guidelines for the reflection positions.[26]

Figure 2 shows the SEM micrographs of the as-synthesized CeO_2, MgO and $MgO{\cdot}CeO_2$ particles. The surface of the CeO_2 powder appears to be rough and highly porous with cavities on the surface between 5 and 8 micron in diameter (Fig. 2a). A close-up image reveals that the bulk material comprises primary particles with either spherical or ellipsoidal shape and Feret diameters between 1.4 and 1.8 (Fig. 2b).

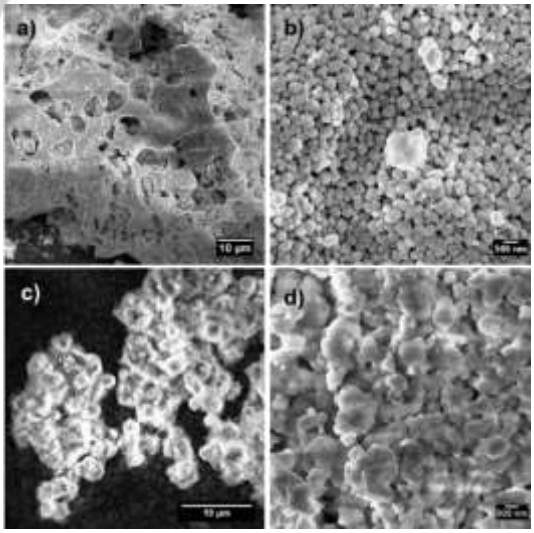

Figure 2. Scanning Electron Microscopy characterization of the particles: a) CeO_2 low magnification and b) high magnification; c) MgO; d) $MgO{\cdot}CeO_2$

Moving to MgO powder, the sample comprises particles with spheroidal shape and mean diameter of 3 μm (Figure 2c).
Every particle appears to be formed by the aggregation of nano-sheets with thickness between 40 and 100 nm (Fig. 2c). The SEM analysis of the $MgO{\cdot}CeO_2$ powder shows that the two materials are closely associated with each other in clusters with diameters between 1 and 5 micron (Fig. 2d). These evidences, taken together with XRD results, suggest that the regular structure and the control on shape and size of the starting materials (MgO and CeO_2) are able to provide a mixed solid oxide of $MgO{\cdot}CeO_2$ with a highly homogeneous structure and phase composition.
The basic/acidic strength of the catalyst can also be controlled by modifying the number of defects in the framework of the material, depending on the calcination temperature used in their synthesis.[27] The influence of the temperature of calcination of $MgO{\cdot}CeO_2$ on the acid-basic sites and BET surface area is shown in Table 3.

Table 3. BET surface area and basicity strength of $MgO{\cdot}CeO_2$ calcined at different temperatures

	Calcination temperature (K)	Total VCO_2 ads (mL/g)	Weak CO_2 ads (mL/g)	Strong CO_2 ads (mL/g)	Total VNH_3 ads (mL/g)	Weak NH_3 ads (mL/g)	Strong NH_3 ads (mL/g)	BET surf area (m^2/g)
1	723	3.62	0.26	3.34	6.11	0.72	5.37	65.4
2	823	3.06	0.28	2.76	3.21	0.69	2.51	66.6
3	923	2.58	0.10	2.43	2.53	0.52	2.01	28.1

The sample calcined at the lowest temperature (723 K) has a larger amount of defect sites, leading to large number of sites of higher basicity, Entry 1.
Raising the calcination temperature to 823 K, the crystal size of CeO_2 grows and the number of defects decreases.[28] As a result, the number of oxygen atoms associated with Ce exhibiting low coordination number decreases, and the number of strong basic sites decreases. Increasing the calcination temperature to 923 K, the strong basic sites further decrease as shown by the value for the absorption of CO_2, which goes to 2.43 mL/g from 3.34 mL/g. At the same time, the weak strength basicity is reduced due to the decrease of the surface area of the $MgO{\cdot}CeO_2$ samples calcined at 923 K.
The lowest temperature of calcination also causes the highest acidity of the solid as it is shown in Table 3 Entry 1, while at the highest temperature of calcination a lower acidity is obtained, even correlated to the drop in the BET surface area, Entry 3.
Therefore, the calcination temperature has a strong effect on both the number and strength of acid and basic sites. In our work, we use the ratio *strong basic to strong acid* sites (n_b/n_a) as a comparison parameter, more than the absolute values, and it works quite well. Noteworthy, moving from 723 to 823 and 923 K the calcination temperature, the ratio n_b/n_a for $MgO{\cdot}CeO_2$ varies from 0.62 to 1.10 and 1.21, indicating an important change in the properties of the catalyst.

2. Study on the stability of DFF *versus* pH

DFF is very sensitive to Broensted basic and/or acidic media. ^{1}H-NMR experiments have clearly shown that acetic acid ([HAc]= 1 mol/L; pH < 3; Fig. 3 A), or NaOH ([NaOH]= 0.001 mol/L; pH>10; Fig. 3 B), deeply affect the stability of DFF in water. Under acidic conditions, conversion to 5-HMF was observed, while under basic conditions several products were formed, among which FFCA and 5-HMF. The tests above confirm that pH has a great influence on the conversion of 5-HMF into DFF, as we have proposed in Scheme 3, and summarize below:

i. Basic sites promote the hydroxyl activation of 5-HMF and get DFF. Nevertheless, high concentration of strong basic centers promote the aldehyde function activation and produce HMFCA instead of DFF,30 Scheme 3b.
ii. Acid pH in the long term affects the stability of DFF in aqueous solution and converts it back to 5-HMF.
iii. The use of external bases increases the system complexity and the separation costs, causing a stronger environmental impact.

However, as an alternative to the use of external soluble acids/bases, we have chosen to use heterogeneous catalysts tunable for their acid/basic properties, in order to perform the oxidation of 5-HMF to DFF with the best conversion and maximum selectivity, making easy its isolation and, avoiding the generation of undesirable waste. Although oxides can be hydrated to produce M-OH moieties, the latter are immobilized on solid particles (*vide infra*) and result to cause lesser pH modification of the medium than soluble Broensted counterparts.

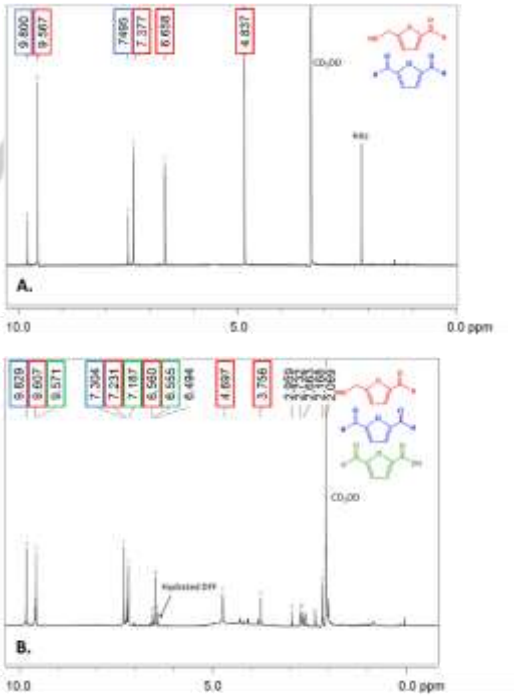

Figure 3. ^{1}H-NMR of the mixture generated by: (A) the addition of HAc to aqueous DFF. (After 12h); (B) the addition of NaOH to aqueous DFF. (After 12h).

Heterogeneous catalysts with an equilibrated distribution of strong acid and basic sites result, thus, to be the most appropriate to perform the conversion of 5-HMF into DFF

3. Catalysts screening in the oxidation of 5-HMF with O_2 in water.

As it is shown in Table 4, MgO (Entry 1) alone affords formic acid (FA) as major product, while, as we have already reported,[22] CeO_2 (Entry 2) shows good selectivity towards FFCA. The oxidation reaction with the mixed oxide, $MgO{\cdot}CeO_2$ calcined at 823 K (Entry 4), gives DFF as almost the sole product with 98% of selectivity accompanied by little by-products.
The conversion depends on the reaction time. To better understand the behavior of the catalyst $MgO{\cdot}CeO_2$, we have carried out studies where parameters such as catalyst composition, P_{O2}, reaction time and temperature were varied.

Table 4. Catalytic tests in the oxidation of 5-HMF using metal oxides as catalysts

	cat	Time (h)	Conv. (%)	Selectivity (mol %)				Basic/ Acid sites[a]
				DFF	HMFCA	FFCA	FA	n_b/n_a
1	MgO	15	23.3	1.8	14.7	0	83.2	2.32
2	CeO_2	15	21.3	0.6	0	88.7	0	0.73
3	$MgO{\cdot}CeO_2$	3	15.1	99	0	0	1	1.10
4	$MgO{\cdot}CeO_2$	15	97.8	98	0	0	2	1.10

Reaction conditions:[5-HMF]i=0.14M, 0.05g of catalyst, PO_2 = 0.9 MPa. T = 373 K. [a]Data from Table 1.

4. Influence of the reaction conditions on the conversion of 5-HMF

Reactions were performed in different conditions of temperature, time, PO_2 and pH as shown in Table 5. Performing the reaction at 373 K (Entry 1) after 3 h DFF was formed as the sole product at low conversion of 5-HMF (15 %) that increased at 15 h (97.8%) keeping selectivity towards DFF at 98%. Under the conditions above, the oxidation of the alcoholic moiety takes place with high selectivity. When the temperature was increased to 403 K, Entry 3, FFCA was obtained as a single product after 9 h of reaction without degradation, indicating the further oxidation of one of the two formyl moieties of DFF into a carboxylic group (Scheme 2).
The oxygen pressure plays also a key role: when it was increased from 0.9 to 2 MPa (Entry 4) poor selectivity was observed. However, when the pressure was dropped to 0.5 MPa (Entry 5) DFF was the only product, but a lower conversion was observed. pH has a great importance in driving the selectivity of the reaction, in fact when the reaction was performed under strong basic conditions (pH >10) with the addition of external bases such as NaOH, Entry 6, HMFCA (57.5%) was preferentially formed and no DFF was detected.

Products derived from the cleavage of the furan ring such as formic acid (FA) and levulinic acid (LA) were also identified and their concentration is function of the reaction conditions. Interestingly enough, the initial concentration of 5-HMF influences the nature of products. The best range for the selective production of DFF is [5-HMF] = 0.15-0.5 M. At lower concentration (<0.1 M) HMFCA is preferentially formed, while at high concentration (> 1 M) FFCA is the dominant product. Such concentration effect is still under investigation in our laboratory.

Table 5. Oxidation of 5-HMF in presence of $MgO{\cdot}CeO_2$ in different conditions.

	cat	t(h)	PO_2 (MPa)	pH T_0	T (K)	Conv (%)	Selectivity (mol %)				
							DFF	HMFCA	FFCA	FDCA	FA/LA
1	$MgO{\cdot}CeO_2$	3	0.9	6	373	15.1	99	0	0	0	<1
2	$MgO{\cdot}CeO_2$	15	0.9	6	373	97.8	98	0	0	0	<2
3	$MgO{\cdot}CeO_2$	9	0.9	6	403	99	0	0	90	0	5
4	$MgO{\cdot}CeO_2$	3	2	6	373	20.6	45.6	0	10.1	0	36.4/ 14.8
5	$MgO{\cdot}CeO_2$	3	0.5	6	373	5.6	99	0	0	0	0
6	$MgO{\cdot}CeO_2$	10	0.9	>10	373	41.8	0	57.5*	2.9	1.7	17.9 (11.2)

Reaction conditions: [5-HMF]i=0.14 M, 0.05 g of catalyst, 7 mL of water. *With external bases.

5. Effect of the composition of the catalyst

The substitution of CeO_2 with another oxidizing agent was tested as it is shown in Table 6.

Table 6. Oxidation of 5-HMF in presence of different mixed oxides based on MgO

	cat	Time (h)	T (K)	Conv. (%)	Selectivity (mol %)				
					DFF	HMFCA	FFCA	FDCA	FA/LA
1	$MgO{\cdot}TiO_2$	9	373	0	0	0	0	0	0
2	$MgO{\cdot}CuO$	3	373	24.04	0	0	82.2	0	0
3	$MgO{\cdot}MnO_2$	9	373	15.7	16.3	0	74.9	0	8.7/1.2
4	$MgO{\cdot}MnO_2$	9	403	98	0	0	64.5	2.6	16.3/12.8

Reaction conditions: $[5\text{-HMF}]_i$=0.14 M, 0.05 g of catalyst, 7 mL of water, PO_2 = 0.9 MPa.

CeO_2 has a crucial role in the reaction: when it was substituted with TiO_2 (Entry 1) the reaction did not proceed. CuO (Entry 2) afforded FFCA, but not DFF. When CeO_2 was substituted with a stronger oxidant oxide such as MnO_2, ($E° Ce^{4+}/Ce^{3+}$=0.40 V; E°

Mn^{4+}/Mn^{2+}=1.23 V, Entry 3), the selectivity towards DFF was dropped because 5-HMF was oxidized to FFCA. When this reaction was carried out at higher temperature, Entry 4, DFF was converted into FFCA and cleavage products such as FA and LA were increased. Small amounts of FDCA were also formed. Catalysts with strong oxidant properties drive, thus, to the further oxidation of DFF. Mixed oxides with increasing amounts of strong basic sites were prepared through the progressive addition of MgO to CeO_2 (Table 7) and each reaction carried out for 3 h.

The composition of the catalyst strongly influences both the conversion yield and the selectivity. Entry 5 (Table 7) shows that increasing the P_{O2} and reaction time promotes the conversion but lowers the selectivity. DFF selectivity is plotted against the ratio Mg/Ce and n_b/n_a in Fig. 4. The yellow points give the selectivity (read on the right Y-axis) and the blue bars give the value of n_b/n_a (read on the left Y-axis); the X-axis gives the composition of the mixed oxides. Starting from 0.1MgO:1CeO_2, MgO content was raised up to 2.2MgO:1CeO_2.

Table 7. Oxidation of 5-HMF in presence of different catalysts synthetized using a different ratio Mg:Ce.

	Cat	t (h)	T (K)	Conv. (%)	Selectivity (mol %)				
					DFF	HMFCA	FFCA	FDCA	FA/LA
1	0.1MgO·CeO_2	3	373	83.0	34.4	23.6	23.5	0	14.8/5.3
2	0.5MgO·CeO_2	3	373	77.8	62.6	0	37.5	0	0
3	1MgO·CeO_2	3	373	15.1	97.0	0	0	0	0
4	2.2MgO·CeO_2	3	373	20.6	80.0	0	0	0	0
5	2.2MgO·CeO_2[a]	9	373	75.0	80.6	0	12.3	0	0

Reaction conditions: $[5\text{-HMF}]_i$=0.14 M, 0.05 g of catalyst, 7 mL of water, PO_2 = 0.9 MPa. [a] PO_2 = 2 MPa.

High conversion was achieved with 0.1MgO:1CeO_2, but the selectivity towards DFF was poor (34% Fig. 5), because further oxidation took place, affording FFCA at 23.5% (Table 7).

Increasing the amount of MgO to 0.5MgO:1CeO_2 (Fig. 4), an increase of the DFF selectivity (62%) was observed, with FFCA still present (37.5% selectivity). Mixed oxide 1MgO:1CeO_2 was the most selective catalyst (98% DFF). However, increasing the amount of MgO from 0.1 to 1 drives to an increase in the selectivity towards DFF; when the amount of MgO was further increased to 2.2 a lower selectivity was obtained but a higher conversion of 5-HMF. As it is shown in Fig. 4, the most effective catalyst for DFF production (MgO·CeO_2) is characterized by a balanced number of strong basic and acid sites on the surface (n_b/n_a=1.1).

However, when the catalyst has a few strong basic and many acid sites (0.1Mg1Ce) the selectivity towards DFF is dropped and FFCA is formed in addition to HMFCA, fact that confirms the hypothesis about the role of basic/acid sites.

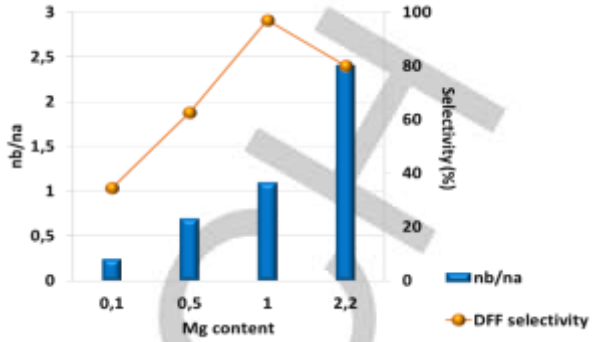

Figure 4. Correlation of selectivity towards DFF (right Y-axis), Mg content (X-Axis) and n_b/n_a of the MgO.CeO_2 catalysts (left Y-axis). Data are taken from Table 7. Catalytic runs were carried out for 3 h at 373 K in all cases. The conversion depends on the catalyst used.

The basicity and acidity of the catalyst has thus a strong influence: the best production of DFF is reached with the catalyst that shows balanced properties in terms of strong basic/acid sites.

6. Effect of the calcination temperature

We have discovered an interesting effect of the calcination temperature over the selectivity (Table 8). We have used MgO·CeO_2 for such experiment as it is the most selective towards DFF. When the solid calcined at 723 K was used, a high selectivity towards FA was observed, Entry 1. With the solid calcined at 823 K (Entry 2) high selectivity towards DFF was obtained. The solid calcined at 923 K produces mainly HMFCA (67%). As discussed above, the n_b/n_a changes with the calcination temperature (Table 3 and 4) influences the selectivity. The solid calcined at lower temperature shows $n_b < n_a$ (n_b/n_a=0.62), which causes the highest production of FA (Table 7, Entry 1).[30] The solids calcined at 823 K shows $n_b \approx n_a$ then the highest production of DFF was achieved. Solids calcined at 923 K have $n_b > n_a$, therefore a high production of HMFCA was observed. It is worth to note that the latter exhibits the same effect of added external bases.

Table 8. Oxidation of 5-HMF in presence of MgO·CeO_2 calcined at different temperatures in 3 h

	Calcination Temperature (K)	Conv. (%)	Selectivity (mol%)				Basic/Acid Sites nb/na
			DFF	HMFCA	FFCA	FA	
1	723	10.6	3.77	0.75	10.37	85.66	0.62
2	823	15.1	99	0	0	<1	1.10
3	923	16.3	16.3	66.56	5.89	20.37	1.21

Reaction conditions: $[5\text{-HMF}]_i$=0.14 M, 0.05 g of catalyst, 7 mL of water, PO_2 = 0.9 MPa

In presence of strongly basic heterogeneous catalysts, thus, the aldehyde moiety becomes strongly involved and either further oxidation of DFF towards FFCA or the oxidation of the aldehydic moiety of 5-HMF towards HMFCA occurs. The results shown above confirm that the chemoselectivity of the reaction is mainly

driven by a combination of strong basic-acidic sites in the catalysts. The use of mixed oxides allows, thus, tune the ratio n_b/n_a in a smooth way, addressing the reaction towards one or the other of the target products.

7. Tests on the recoverability and recyclability of the catalyst

The catalyst recovery and reusability was tested by using either 2.2MgO·CeO_2 (Fig. 5) or MgO·CeO_2. After each reaction run, the catalyst was filtered off, washed with water (7 mL) three times, and either used directly or calcined at 823 K and then reused in a new run. Already at the second cycle of reaction using 2.2MgO·CeO_2 reduction of DFF yield was evident (Fig. 5), while a significant loss of the weight of the catalyst was verified. EDX analyses on the recovered catalyst did show a loss of MgO and the increase of the ratio Ce/Mg: before the catalytic run it was 0.45 after the first run was 0.76. It is interesting to note that after the loss of Mg the catalysts was more robust for the consecutives runs, the selectivity of DFF was kept constant (> 90%) for two more runs.

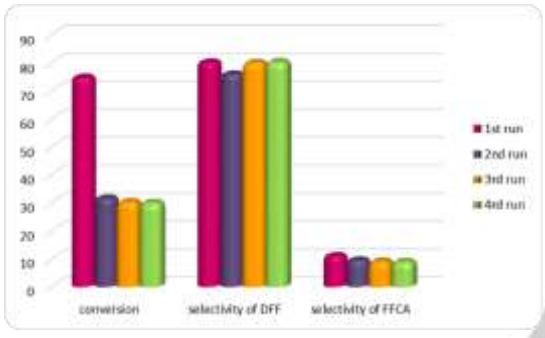

Figure 5. Study on the reusability of 2.2MgO·CeO_2 (9 h cycle)

The loss of Mg moved the composition of the catalyst towards the 1:1 ratio with increase of stability and good selectivity towards DFF.

By contrast, when MgO·CeO_2 was used as catalyst the performance was constant even after repeated use (98% selectivity towards DFF at 98% conversion). The catalyst was calcined after each use. After three cycles of reaction, the reduction of DFF yield was very limited (<9%) relative to the first cycle. Also, no loss of weight of the catalysts was detected after its use.

7.1. Catalysts recycling: experiments and characterization by XPS and XRD

Catalysts MgO·CeO_2 and 2.2MgO·CeO_2 were further characterized by XPS and XRD to better clarify changes in their structure/composition during a catalytic cycle.

XPS analysis of the 2.2MgO·CeO_2 sample before and after catalysis did show a decrease of the surface content of Ce(IV) and MgO after the reaction. The reduction of Ce(IV) was due to the formation of Ce(III) (13% of Ce(III) was found on the surface, that decreased after calcination). There were no differences on the oxidation state of Mg before and after reaction, as expected.

XRD analysis was also performed on the solid before and after reaction. For MgO·CeO_2, the pattern C in Fig. 1 is dominated by CeO_2 reflections with some contribution from MgO. The XRD pattern of the solid after the catalytic run (green line in Fig. 6) shows that the reflections due to MgO at *ca*. 43° (200) and ca 62° (220) are not present, whereas a new reflection appears at *ca*. 38° that corresponds to the most intense reflection of $Mg(OH)_2$, the second most intense reflection being present at *ca.* 58°, where a shoulder to the 222 reflection of CeO_2 (Fig. 6) can be observed.[31]

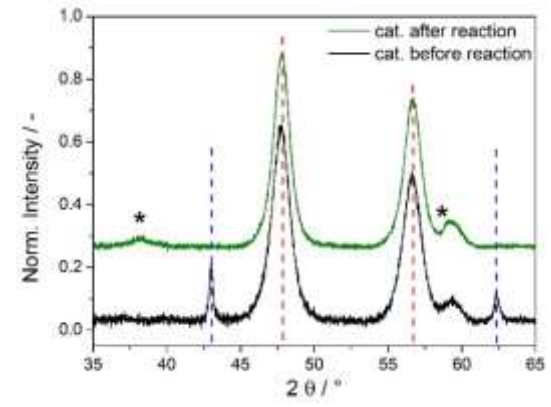

Figure 6. XRD of MgO·CeO_2 before and after a catalytic run. The blue dashed vertical lines indicate the reflections of MgO that are missing in the solid after the reaction. A new reflection appears at *ca.* 38°(*), suggesting the presence of $Mg(OH)_2$. The red dashed vertical lines refer to CeO_2 reflections.

This result, taken together with the elemental analysis, suggests that the MgO is not leached during the reaction but converted into $Mg(OH)_2$ that is still present in the catalyst. $Mg(OH)_2$ can be formed by the reaction with solvent water, in agreement with what reported by other authors.[31,32] Calcination of the solid after the catalytic cycle regenerates MgO·CeO_2 by dehydration of $Mg(OH)_2$ to MgO and re-establishes its activity. The powder after the catalytic cycle was analyzed by SEM, finding that the morphology and size of the particles were not considerably different from those of the as-synthesized powders (Fig. 2d). Noteworthy, that MgO or $Mg(OH)_2$ is not lost during the catalytic run is demonstrated by EDX that shows that Mg is not present in solution or is present at trace level. This allows the catalyst MgO.CeO_2 recover its efficiency and performance after calcination. The results discussed above demonstrate that MgO.CeO_2 is an active, recoverable, recyclable and selective catalyst in the aerobic oxidation of 5-HMF into DFF (98% conversion, 99% selectivity) or FFCA (99% conversion, 90% selectivity), depending on the reaction temperature, in water, without generation of extra waste in the process, fully responding to the principles of sustainable chemistry.

Conclusions

The non-precious mixed oxide $MgO{\cdot}CeO_2$ prepared by the simple HEM method was used as effective catalyst in the selective oxidation of 5-HMF (0.14 to 0.5 M) to DFF using water as solvent, O_2 as oxidant, without any type of additives. In this work we have also demonstrated that the reaction parameters can be modulated to oxidize the aldehyde moiety of 5-HMF instead. The key role of basic/acidic sites has been proved. To reach the maximum selectivity towards DFF, an almost equal number of strong basic and acid sites is required. Relationship between initial concentration of 5-HMF and selectivity or conversion has also been demonstrated. Working at low concentration of substrate (0.02 M) and increasing the basicity of the catalyst, HMFCA is preferentially obtained. The composition of the catalyst plays a key role: to reach more than 98% of selectivity towards DFF, $1MgO{:}1CeO_2$ is needed. We have clearly shown in this paper that $MgO{\cdot}CeO_2$ is recoverable and reusable in next catalytic runs after a calcination step. Transient deactivation is due to hydration of MgO to $Mg(OH)_2$, as shown by XRD, more than to modification of the composition by leaching. The process that we have discussed in this work is totally eco-friendly and no secondary residues have been obtained in optimized conditions. This makes the catalyst a good candidate for an eventual up-scale.

Experimental Section

Experimental Details

1. Materials

Cerium ammonium nitrate ≥98% (by titration); cerium (IV) oxide nanopowder, <25 nm particle size 99.95% trace rare earth metals basis; magnesium oxide 99.99% trace metal basis; magnesium (II) nitrate hexahydrate 99%; 2,5-furandicarboxaldehyde ≥97%; 5-formyl-2-furoic acid 99%; 5-hydroxymethyl-2-furancarboxylic acid 99%, were ACS grade reagents purchased from Sigma Aldrich. 5-(hydroxymethyl)furfural was prepared as we have reported in ref. 2a,b.

2. Catalysts preparation

a) Synthesis of $MgO{\cdot}CeO_2$:

Cerium (IV) ammonium nitrate and magnesium (II) nitrate hexahydrate (the relative mass depends on the desired ratio Mg/Ce in the final mixed oxide: in the case of $MgO{\cdot}CeO_2$, 0.43 g of Ce(IV) ammonium nitrate were reacted with 0.25 g of Mg(II) nitrate hexahydrate) were mixed in a High Energy Milling-HEM apparatus and pulverized at 790 rpm during 1h with pause of 1 min every 15 min and inversion of the rotation sense. The pale yellow mixture was calcined for 3 h at 723-923 K giving a yellow solid. The solid was transferred into a flask and stored under N_2 atmosphere to prevent uncontrolled surface deterioration prior to catalysis.

b) Synthesis of $MgO{\cdot}M_nO_m$: (M=Ti, Cu, Mn)

An equivalent number of mmol of magnesium (II) nitrate hexahydrate and the nitrate or oxide of the desired oxidant (depending on the commercial availability of the solids: for example for the synthesis of $MgO{\cdot}TiO_2$, 0.25 g of magnesium (II) nitrate hexahydrate were reacted with 0.079 g of TiO_2, more details are shown in Table 9), were mixed in a High Energy Milling-HEM apparatus and treated as reported in (a). The mixture was calcined for 3 h at 723 K giving a solid which color depends on the compounds mixed. The calcined solids were transferred into a flask and stored under N_2 atmosphere to prevent uncontrolled surface deterioration prior to catalysis.

Table 1. Mass (g) used for the synthesis of the mixed oxides

Entry	Mixed Oxide	g $Mg(NO_3)_2{\cdot}7H_2O$	g other nitrate/oxide
1	$MgO{\cdot}TiO_2$	0.25	0.079 TiO2
2	$MgO{\cdot}CuO$	0.25	0.19 $Cu(NO_3)_2{\cdot}3H_2O$
3	$MgO{\cdot}MnO_2$	0.25	0.087 MnO_2

3. Catalytic tests

The conversion of 5-HMF at a fixed temperature was studied in a 50 mL stainless-steel reactor equipped with a withdrawal valve and an electrical heating jacket. An appropriate amount of 5-HMF, depending on the desired concentration, was dissolved in 7 mL of distilled water in a glass reactor containing a magnetic stirrer, and 0.05 g of the catalyst under study were added. The glass-reactor was then transferred into the autoclave that was closed and purged three times with O_2.

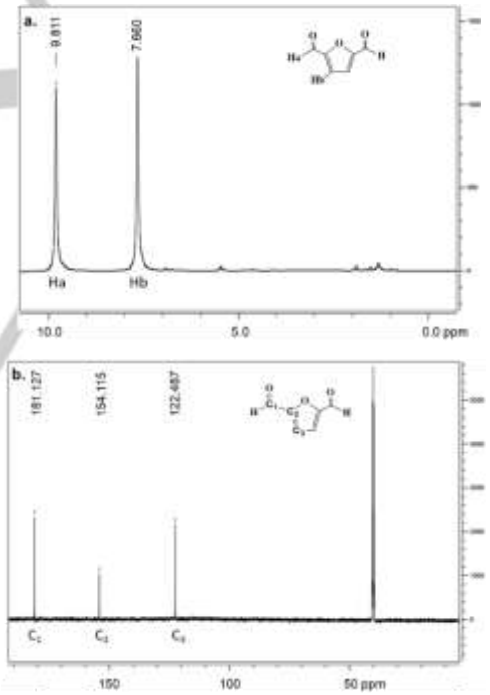

Figure 7. a. ^{1}H-NMR, b. ^{13}C-NMR of isolated DFF in $CDCl_3$ (Bruker, 600 MHz) at 300 K.

It was charged with the appropriate pressure of oxygen and heated to the reaction temperature as specified in Results and Discussion. At fixed intervals of time, stirring was stopped so to allow the solid to settle, a 0.1 mL sample was withdrawn and analysed by HPLC following the conversion of 5-HMF. When the concentration of the latter dropped to a constant value (or even zero), the reaction was stopped. The solution and the solid were

separated by centrifugation and both extracted three times with 7 mL of ethyl acetate (EtOAc), collecting the EtOAc phases. Such procedure was necessary because DFF is only slightly soluble in water and can precipitate in the reaction medium or even deposit on the catalyst. The EtOAc phase was washed with water to remove the residual 5-HMF eventually dissolved into it, dried with Na_2SO_4, filtered and analysed by GC. Evaporation in vacuum of EtOAc gave the pure DFF (isolated yield: 98%) which was analysed by NMR (Figure 7). Spectra show that DFF is very pure, with only very minor traces of by-products. It is worth to emphasize that increasing the amount of catalyst, speeds-up the reaction, but leaves unchanged the selectivity.

4. Analytical methods

5-HMF and derivatives were analysed by using a JASCO HPLC equipped with a Refractive Index (RI) detector and a Phenomenex Rezex RHM Monosaccharide H^+(8%) 300x7.8mm at 343 K. A 0.005 N water solution of sulphuric acid was used as the mobile phase. The flow rate was between 0.5-0.9 mL/min. The concentration of residual 5-HMF and reaction products were determined using a RI detector. DFF concentration was analysed in ethyl acetate solution, using a Thermo Scientific GC with initial temperature of 323 K for 2 min. The rate of the first ramp was 7 º/min until 393 K for 8 min. The second ramp rate was 15 º/min until 403 K for 10 min.

Pulse ChemiSorb 2750 Micromeritics instrument was used for the surface characterization of the catalysts. Analyses of the acidic/basic sites were carried out using NH_3 or CO_2, respectively, as probe-gas using 100 mg of catalyst. The samples were pre-treated under N_2 (30 mL min-1) flow at 673 K. The Pulse Chemisorb was performed with NH_3 or CO_2 gas using He as carrier gas (30 mL min-1). Brunauer Emmett Teller (BET) surface area was determined using N_2/He as carrier gas at 273 K followed by heating up to 923 K. Temperature Programmed Desorption (TPD) were performed under He flow at 30 mL min-1.

All reported values are the average of three measurements, with a standard deviation < 3%.

X-Ray Diffraction (XRD) analysis was performed using a D8 Advance instrument (Bruker AXS GmbH, Germany) with Cu Kα radiation (λ = 1.5406 Å). The patterns were collected in the 2θ range of 20-80° (step size 0.014°, 2 seconds). The powders were manually compressed inside low volume sample holders comprising low background sample cups with a vicinal (911) Si crystal of 25 mm diameter (Bruker AXS GmbH). All the presented patterns were background subtracted. X-ray photoelectron spectroscopy (XPS) was conducted on a Thermo VG scientific ESCA MultiLab-2000 spectrometer with a monochromatized Al-Kα source (1486.6 eV) at constant analyser pass energy of 25 eV.

ULTRA™ 55 instrument (Carl Zeiss AG, Germany) was used for Scanning Electron Microscopy (SEM) analyses. The particles were deposited directly on a conductive sticky carbon pad (Plano GmbH). Image analysis was performed by using the freely available software.[33] The size of particles with ellipsoidal morphology was estimated through the Feret´s diameter, i.e. as ratio between the projection of the long and short axis in electron micrographs.

Energy Dispersion X-ray Spectrometer (EDX) Shimadzu EDZ-720 was used for elemental analyses of the catalysts.

Acknowledgements

The work was funded by the MIUR Industrial Research Project CTN01_00063_49393 “REBIOCHEM” in the frame of the Operative National Program-Research and Competitiveness 2007-2013. VALBIOR is gratefully thanked for gracious use of equipment.

Keywords: Oxidation of 5-HMF • selective non-precious catalysts • aerobic oxidation in water• 2,5-diformylfuran (DFF) • 2-formyl-5-furancarboxylic acid (FFCA).

[1] a) S. Shafiee, E. Topal, *Energy Policy* **2009**, *37*, 181-189; b) M. Höök, X. Tang, *Energy Policy* **2013**, *52*, 797-809.

[2] a) A. Dibenedetto, M. Aresta, L. di Bitonto, C. Pastore, *ChemSusChem* **2016**, *9*, 118-125; b) A. Dibenedetto, M. Aresta, C. Pastore, L. di Bitonto, A. Angelini, E. Quaranta, *RSC Adv.* **2015**, *5*, 26941- 26948; c) W. Deng, Q. Zhang, Y. Wang, *Sci. China-Chem.* **2015**, *58*, 29-46; d) X.L. Tong, Y. Ma, Y.D. Li, *Appl Catal A: Gen* **2010**, *385*, 1-13.

[3] a) M. Besson, P. Gallezot,C. Pinel, *Chem. Rev.* **2014**, *114*, 1827-1870; b) R.-J. van Putten, J.C. van der Waal, E. de Jong, C.B. Rasrendra, H.J. Heeres, J.G. de Vries, *Chem. Rev.* **2013**, *113*, 1499-1597; c) B. Xiao, M. Zheng, X. Li, J. Pang, R. Sun, H. Wang, X. Pang, A. Wang, X. Wang, T. Zhang, *Green Chem.* **2016**, *18*, 2175-2184.

[4] a) K. T. Hopkins, W.D. Wilson, B.C. Bender, D.R. McCurdy, J.E. Hall, R.R. Tidwell, A. Kumar, M. Bajic, D.W. Boykin, *J. Med. Chem.* **1998**, *41*, 3872-3878; b) D.W. Boykin, A. Kumar, J. Spychala, M. Zhou, R.J. Lombardy, W.D. Wilson, C.C. Dykstra, S.K. Jones, J.E. Hall, R.R. Tidwell, C. Loughton, C.M. Nunn, S. Neidle, *J. Med. Chem.* **1995**, *38*, 912-916.

[5] M. Del Poeta, W.A. Schell, C.C. Dykstra, S.K. Jones, R.R. Tidwell, A. Kumar, D. W. Boykin, J. R. Perfect, *Antimicrob. Agents Chemother.* **1998**, *42*, 2503-2510.

[6] a) A.S. Amarasekara, D. Green, L.D. Williams, *Eur. Polym. J.* **2009**, *45*, 595-598; b) A. Gandini, N.M. Belgacem, *Polym. Int.* **1998**, *47*, 267-276.

[7] D.T. Richter, T. D. Lash, *Tetrahedrom Lett.* **1999**, *40*, 6735-6738.

[8] a) B. Karimi, H.M. Mirzaei, E. Farhangi, *Chem.Cat.Chem* **2014**, *6*, 758-762; b) Y. Zhu, M. Shen, Y. Xia, M. Lu, *Catal. Comm.* **2015**, *64*, 37-43; c) R. Fang, R. Luque, Y. Li, *Green Chem*. **2017**, 19, 647-655.

[9] a) D. Prat, A. Wells, J. Hayler, H. Sneddon, C.R. McElroy, S. Abou-Shehada, P.J. Dunn, *Green Chem.* 2016, 18, 5082-5085; b) H. Zhang, Q. Wu, C. Guo, Y. Wu, T.Wu, *ACS Sust Chem and Eng,* **2017**, *5*, 3517-3523; c) P.V. Rathod, S.D. Nale, V.H. Jadhav, *ACS Sust Chem and Eng*, **2017**, *5(1)*, 701-707; d) J., Li, G. Lv, B. Lu, Y. Wang, T. Deng, X. Hou, Y. Yang, *Energy Technology*, **2017**, *5*, 1429-1434; e) G. Li, Z. Sun, Y. Yan, Y. Zhang, Y. Tang, *ChemSusChem*, **2017**, *10*, 494-498.

[10] a) Nie, J.; Xie, J.; Liu, H. *J. Catal.* **2013**, *301*, 83-91; (b) Antonyraj, C. A.; Jeong, J.; Kim, B.; Shin, S.; Kim, S.; Lee, K.-Y.; Cho, J. K. *J. Ind. Eng. Chem.* **2013**, *19*, 1056-1059; (c) Stahlberg, T.; Eyjolfsdottir, E.; Gorbanev, Y. Y.; Sadaba, I.; Riisager, A. *Catal. Lett.* **2012**, *142*, 1089-1097; (d) Takagaki, A.; Takahashi, M.; Nishimura, S.; Ebitani, K. *ACS Catal.* **2011**, *1*, 1562-1565.

[11] F. Neaţu, N. Petrea, R. Petre, V. Somoghi, M. Florea, V.I. Parvulescu, *Catal. Today* **2016**, *278*, 66-73.

[12] D.X. Martinez-Varga, J. Rivera de la Rosa, L. Sandoval-Rangel, J.L. Guzman-Mar, M.A. Garza-Navarro, C.J. Lucio-Ortiz, D.A. De Haro-DelRio, *Applied Cat A: General*, **2017**, *547*, 132-145.

[13] J. Chen, J. Zhong, Y. Guo, L. Chen, *RSC Adv.* **2015**, *5*, 5933-5940.

[14] J. Artz, S. Mallmann, R. Palkovits, *ChemSusChem* **2015**, *8*, 672-679.

[15] J. Nie, J. Xie, H. Liu, *Cuihua Xuebao* **2013**, *34*, 871- 875.

[16] Y.Y. Gorbanev, S. Kegnaes, A. Riisager, *Top. Catal.* **2011**, *54*, 1318-1324.

[17] Y. Yan, X. Tong, K. Wang, X. Bai, *Catal. Commun.* **2014**, *43*, 112-115.

[18] a) X. Wan, C. Zhou, J. Chen, W. Deng, Q. Zhang, Y. Yang, Y. Wang, *ACS Catal.* **2014**, *4*, 2175-2185; b) S. Albonetti, A. Lolli, V. Morandi, A. Migliori, C. Lucarelli, F. Cavani, *Appl. Catal., B* **2015**, *163*, 520-530; c) A. Villa, M. Schiavoni, S. Campisi, G.M. Veith, L. Prati, *ChemSusChem* **2013**, *6*, 609-612.

[19] F. Tao, Y. Cui, P. Yang, Y. Gong, *Russ. J. Phys. Chem. A* **2014**, *88*, 1091-1096.

[20] a) S. Li, K. Su, Z. Li, B.Cheng, *Green Chem.* 2016, 19, 914-918; b) Z. Zhang, J. Zhen, B. Liu, K. Lv, K. Deng, *Green Chem.* **2015**, *17*, 1308-1317; c) L. Zheng, J. Zhao, Z. Du, B; Zong, H. Liu, *Science China Chemistry*, **2017**, *60*, 950-957; d) S. Xu, P. Zhou, Z. Zhang, C. Yang, B. Zhang, K. Deng, S. Bottie, H. Zhu, *J Am Chem Soc*, **2017**, *139*, 14775-14782.

[21] X.L. Tong, Y. Ma, Y.D. Li, *Appl. Catal. A-Gen*. **2010**, 385, 1-13.

[22] a) M. Ventura, M. Aresta, A. Dibenedetto, *ChemSusChem* **2016**, *9*, 1096-1100; b) M. Aresta, A. Dibenedetto, M. Ventura, Patent 102016000014339, **2016**; c) M. Ventura, A. Dibenedetto, M. Aresta, *Inorg. Chim. Acta*, **2018**, *470*, 11-21.

[23] G.A.H. Mekhemer, S.A. Halawy, M.A. Mohamed, M.I. Zaki, J. *Phys. Chem. B* **2004**, *108*, 13379-13386.

[24] P. Carniti, A. Gervasini, F. Bossola, V.D. Santo, *Appl. Catal. B: Environm*. **2016**, *193*, 93-102.

[25] S.V. Chavan, A.K. Tyagi, *Thermochim. Acta* **2002**, *390*, 79-82.

[26] A. Kumar, S. Thota, S. Sivakumar, S. Priya, J. Kumar, *J. Sol-Gel Sci. Technol* **2013**, *68*, 46-53.

[27] Q. Dai, X. Wang, G.Lu, *Appl. Catal. B: Environm.* **2008**, *81*, 192-202.

[28] V.V. Pushkarev, V.I. Kovalchuk, J.L. d'Itri, *J. Phys. Chem. B* **2004**, *108*, 5341-5348.

[29] H. Ait Rass, N. Essayem, M. Besson, *Green Chem.* **2013**, *15*, 2240-2251.

[30] S.K. Triantafyllidis, A.A. Lapas, M. Stöcker, *The role of catalysis for the sustainable production of bio-fuels and bio-chemicals*; Elsevier, 2013.

[31] M. Uda, H. Okuyama, T.S. Suzuki, Y. Sakka, *Sci. Tech. Adv. Mat.* **2012**, *13*, 025009.

[32] F. Al-Hazmi, A. Umar, G.N. Dar, A.A. Al-Ghamdi, S.A. Al-Sayari, A. Al-Hajry, S.H. Kim, R.M. Al-Tuwirqi, F. Alnowaiserb, F. El-Tantawy, *J Alloys Compd* **2012**, *519*, 4-8.

[33] W.S. Rasband, J. Image, *U.S. National Institutes of Health*, Bethesda, Maryland, USA, http://imagej.nih.gov/ij/, 1997–2014.

10.1002/cssc.201800334

WILEY-VCH

FULL PAPER

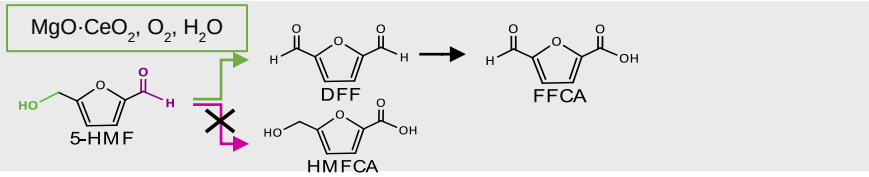

By using a tunable mixed oxide such as $MgO{\cdot}CeO_2$ we have obtained a selective and quantitative oxidation of 5-HMF to DFF (or FFCA) in water in the presence of O_2 as oxidant. Interestingly, the oxidation of the aldehyde moiety, which brings to the formation of HMFCA, is suppressed.

Maria Ventura, Francesco Lobefaro, Elvira de Giglio, Monica Distaso, Francesco Nocito, and Angela Dibenedetto

Page No. – Page No.

Selective aerobic oxidation of 5-(hydroxymethyl)furfural to 2,5-diformylfuran or 2-formyl-5-furancarboxylic acid in water using $MgO{\cdot}CeO_2$ mixed oxides as catalysts

[a] Prof. A. Dibenedetto, Prof. E. de Giglio, Dr F. Nocito
Department of Chemistry,
University of Bari, Campus Universitario, 70126 Bari, Italy
E-mail: angela.dibenedetto@uniba.it
[b] Prof. A. Dibenedetto, Dr M. Ventura
CIRCC, Via Celso Ulpiani, 27, 70126 Bari, Italy